[10] Eaton, R. R., "Numerical and Experimental Surface Pressure Distributions and Shock Shapes On 15-Degree Sphere Cones at Angles of Attack," SC-DR-69-0259, 1969, Sandia Labs., Albuquerque, N. Mex.
[11] Ashurst, W. T., "HANDY," SCL-DR-70-25, March 1970, Sandia Labs., Livermore, Calif.
[12] Babenko, K. I. et al., "Three-Dimensional Flow of Ideal Gas Past Smooth Bodies," TT-F-380, April 1966, NASA.
[13] Kryvoruka, J. K. and Ashurst, W. T., "Re-Entry Vehicle Finned Roll Rate Control: Aerodynamic and Flight Dynamic Analysis," AIAA Paper 73-183, Washington, D.C., 1973.
[14] Rakich, J. V. and Cleary, J. W., "Theoretical and Experimental Study of Supersonic Steady Flow around Inclined Bodies of Revolution," *AIAA Journal*, Vol. 8, No. 3, March 1970, pp. 511–518.
[15] George, O. L., Jr., "An Experimental Investigation of the Flow Field Around an Inclined Sharp Cone in Hypersonic Flow," SC-RR-69-577, Sept. 1969, Sandia Labs., Albuquerque, N. Mex.
[16] Kryvoruka, J. K., "A Formulation of the Equations of Motion for Flight Vehicles with Semi-Passive Roll Control Systems," SCL-RR-720007, April 1972, Sandia Labs., Livermore, Calif.
[17] Fail, R. and Garner, H. C., "Calibration Models for Dynamic Stability Tests," Rept. 563, 1968, Advisory Group for Aerodynamic Research and Development, Neuilly-sur-Seine, France.

MARCH 1974 J. SPACECRAFT VOL. 11, NO. 3

A Wind-Tunnel Study of Spinning Conical Disk Decelerators at Mach 4

ANTONI K. JAKUBOWSKI *
Virginia Polytechnic Institute and State University, Blacksburg, Va.

An experimental investigation was made of the aerodynamic torque and drag characteristics of several configurations of rotating conical disk models placed in a supersonic Mach 4 stream. A basic shape of 73° half angle was used and solid surface configurations as well as "porous" ones were tested. Experiments seem to indicate that at a given supersonic Mach number, the torque coefficient of a highly porous configuration can be approximately expressed as a function of a single variable parameter (Reynolds number related to the peripheral velocity) and two constants which depend on geometry of the disk. For a selected geometric configuration, torque coefficient is inversely proportional to the porosity of the surface. For solid surface disks, torque increases rapidly when grooves (or other "deformations") are present which are oriented in the radial direction. Circumferential grooves or slots produce only a relatively small torque increase. A suggestion is made about an aerodynamically "optimal" network of a spinning filamentary decelerator. Drag coefficient of rotating disks varies consistently with the degree of porosity. Within the range of spin rates tested, C_D remained constant, independent of rotation.

Nomenclature

A = reference area (maximum cross-sectional area of disk) πR^2
A_o = open surface area of disk
A_t = total surface of leading side of disk
C_D = drag force coefficient, $D/q_\infty A$
C_M = aerodynamic drag torque coefficient, $M_d/(\rho_\infty/2)\omega^2 R^5$
D = drag force
M = freestream Mach number
M_d = aerodynamic torque of conical disk (for porous configuration) or friction torque on the leading side of disk (for solid surface configuration)
q_∞ = freestream dynamic pressure
r = radius
R = maximum radius of disk
Re = Reynolds number
s = spin rate parameter, $\omega R/U$
U = freestream velocity
v = circumferential velocity in boundary layer
z = distance perpendicular to surface
λ = geometric porosity
μ = viscosity
ν = kinematic viscosity
ρ = density
ρ_∞ = freestream density
τ = shearing stress
ϕ = half-angle of conical disk
ω = angular velocity

Received June 8, 1973; revision received October 19, 1973. This work was supported by the VPI & SU Research Division Grant. The author wishes to thank J. Lukasiewicz for his advice and interest in this study and J. Van Overeem and W. A. Shirley for their assistance in the experimentation.
Index categories: Entry Deceleration Systems and Flight Mechanics (e.g. Parachutes); Supersonic and Hypersonic Flow.
* Assistant Professor, Aerospace Engineering. Member AIAA.

Introduction

A SPINNING flexible disk has been proposed[1,2] as a potential entry decelerator which offers many operational advantages such as large drag area combined with low decelerator weight fraction, effective radiation cooling, improved communication throughout the descent, and a potential for maneuvering. Such a decelerator can be formed, for instance, by a rapidly spinning filamentary disk mounted at its center to a hub on the nose of the capsule and maintained in an erected position by the centrifugal forces. The energy for the initial spin-up can be provided by small rocket motors mounted on the rim of the disk. For missions requiring maneuvering, the periphery of the disk may be equipped with a number of aerodynamic vanes to counteract the aerodynamic friction torque of the disk.

Aerodynamic analysis of a spinning disk decelerator requires

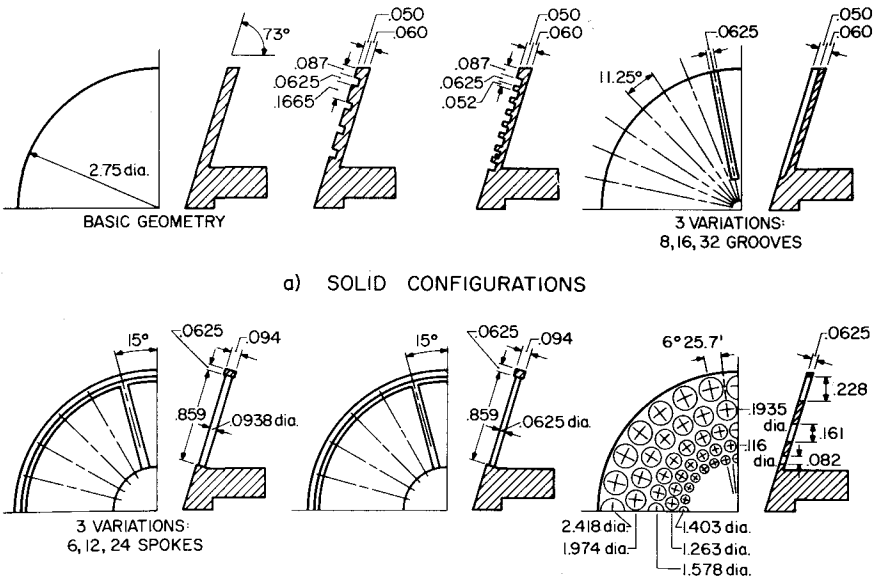

Fig. 1 Geometry of the disk models (dimensions are given in inches).

knowledge of aerodynamic torque at hypersonic and supersonic speeds, the effects of porosity, heating distribution in nonaxial flight and the performance characteristics of rim vanes for driving torque and flutter suppression. Available literature on the subject is scarce and deals mainly with the mechanics of the filamentary disk and its flight dynamics.[1-4] The main purpose of this investigation was to obtain basic characteristics of aerodynamic torque of spinning conical disks of several configurations (including nonporous conical-disks) at a supersonic forward speed. The tests were conducted in an axial flow at Mach number of 4 and at test section Reynolds numbers around 13.6×10^6/ft. All models had a diameter of 2.75 in. and the rotation was varied from 600 rpm to 14,500 rpm.

Apparatus

Wind Tunnel and Models

The investigation was performed in the VPI & SU 9×9 in. supersonic wind tunnel. The tunnel is an intermittent blowdown-type facility and can be operated at a maximum initial pressure of about 150 psi. Geometry of the models tested is shown in Fig. 1 and a view of a model in the test section is shown in Fig. 2. All models started with a basic conical shape with half-angle of 73°.† The size of the smooth, conical nose portion of the models was determined by design and fabrication considerations and at the same time it may "simulate" the front surface of a payload. The porous configurations tested included a perforated surface and five variations of rotor net-type disks, where the porosity was varied by varying the number and size of the spokes. The solid configurations included a smooth surface (for comparison purposes and to evaluate the effect of drag force), surfaces with 4 and 8 concentric circular grooves, and surfaces with 8, 16, and 32 evenly spaced radial grooves.

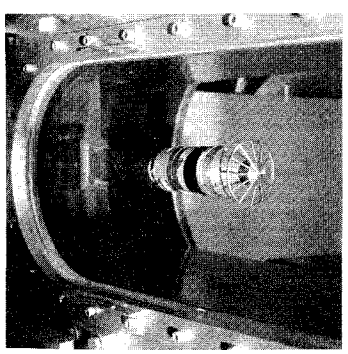

Fig. 2 View of a model in the test section.

† We assume that during a supersonic phase of deceleration the half-angle of a flexible spinning disk would be between 70° and 80°.

Instrumentation and Procedure

The models were driven by a precision permanent magnet d.c. motor made by Globe Industries (type GRP). Spin rate was varied by regulating the supply voltage. The front and back parts of the motor were completely redesigned and modified to accommodate speed and drag measuring units. Speed measuring unit consisted of an iron gear mounted on the shaft of the motor and a miniature magnetic pick-up attached to the frame of the motor. The voltage impulses produced by the rapidly varying magnetic flux (as the motor is turned on) were amplified and then counted by an analyzer and stored in its memory. After each test the memorized data were automatically printed out giving a very precise record of the angular frequency, ω. The drag force, D, was measured by means of a strain-gauge, temperature compensated element installed behind the motor shaft.

The following quantities were recorded continuously during each run: stagnation pressure and temperature, motor supply voltage, armature current, spin rate and drag force. Torque values were obtained graphically by using motor performance characteristics. The latter were determined experimentally and were checked several times over the period of experimentation. The torque required to overcome friction of the motor-balance system itself, i.e., at no external load, was accounted for in the calibration. Therefore, the torque values established from the calibration curves represented the torque produced by the aerodynamic friction of the model and a possible contribution due to a drag force. This latter contribution, caused by the friction in the thrust ball bearing at the aft end of the motor shaft, was calculated for each run from the magnitude of the measured drag force (using a "friction coefficient" assumed equal to 0.0018[5]) and was found to be very small for most of the tests (less than 1.5% of the measured aerodynamic torque). In addition to force measurements, schlieren photographs of spinning disks were made and used for qualitative examination of the flowfield past the disks.

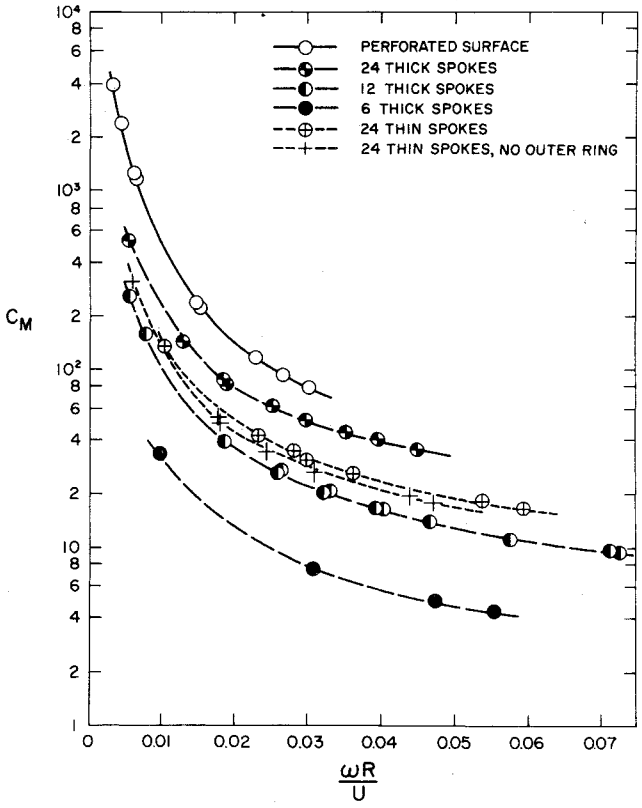

Fig. 3 Torque coefficient vs spin rate parameter; porous surfaces.

Results and Discussion

The results are presented in terms of the following dimensionless parameters: torque coefficient $C_M = M_d/(\rho_\infty/2)\omega^2 R^5$, spin rate parameter $s = \omega R/U$, Reynolds number $Re_d = \omega R^2/\nu$, and geometric porosity $\lambda = A_o/A_t$.

Porous Configurations

Figure 3 shows torque coefficient vs spin rate parameter for porous configurations. As expected, the torque coefficient changes very rapidly with the degree of porosity and the geometry of the disk. For geometrically similar disks, the torque coefficient varies linearly with the porosity. This can be seen in Fig. 4 where C_M is plotted against λ for the models with spokes. The porosity was varied by using different numbers and two

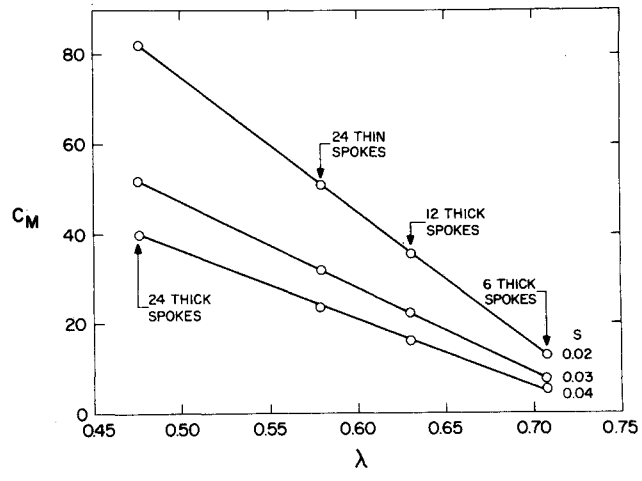

Fig. 4 Torque coefficient vs geometric porosity; disks with spokes.

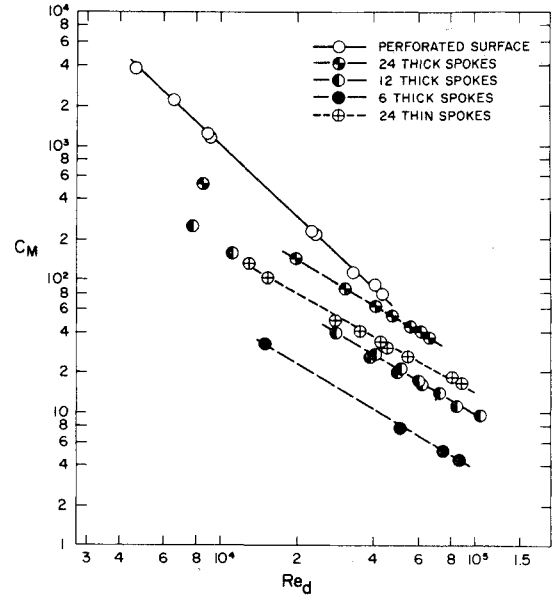

Fig. 5 Torque coefficient vs Reynolds number; porous configurations.

different sizes of the spokes. Geometrical pattern of the surface has a very strong effect on C_M. For instance, the perforated disk and the disk with 24 thick spokes have nearly the same porosity (0.478 and 0.475, respectively), yet C_M of the perforated surface is much larger than C_M of the 24-spoke model. In the case of a perforated surface, we may expect that C_M will depend on factors like the thickness of the disk wall, size and direction of the holes, etc. The turning moment of a porous disk may be thought of as resulting from the two main contributions. The first one, which is increasingly dominant with λ, is due to the momentum drag of the flow through the disk. The second contribution, which is dominant at low λ, is the friction torque due to the velocity gradient in the boundary layer on the leading surface of the disk. The flow along the front surface is due to the main flow which is identical with the case of a nonspinning model and due to the centrifugal effects. The particles which rotate with the boundary layer are thrown outwards owing to the existence of centrifugal forces. Both abovementioned contributions to the turning moment increase with the angular velocity ω resulting in a rapid increase of torque.

Plotting C_M vs Reynolds number related to peripheral velocity of the disk, $\omega R^2/\nu$, shows that with few exceptions, the data collected for a particular configuration follow a straight line on a log-log graph (Fig. 5). Few points that are considerably off, correspond to low spin rates and may indicate that a linear presentation breaks down for an extended Re_d-range. They might also indicate the presence of a kind of "fine dependence" on spin rate parameter. That is that in addition to a dominant dependence of C_M on Re_d, there may be some independent and small variation of C_M with the spin rate parameter (i.e., at Re_d = const), with an effect becoming significant at very low rotations. To discuss this effect, the spin rate parameter should be rather defined in terms of a velocity behind the shock, for instance, the velocity behind the normal shock. Experimental verification of this effect would require an independent variation of ω and Re_d, which was not possible in this study. Nevertheless, at least over a fairly large range of spin rates,‡ a linear dependence of log C_M vs log Re_d can be approximately assumed suggesting an empirical equation for C_M for any particular configuration

$$C_M = b(Re_d)^a$$

where a and b are constants readily obtainable from Fig. 5.

‡ Spin rates in excess of 0.1 seem to be unrealistic for a decelerator application.

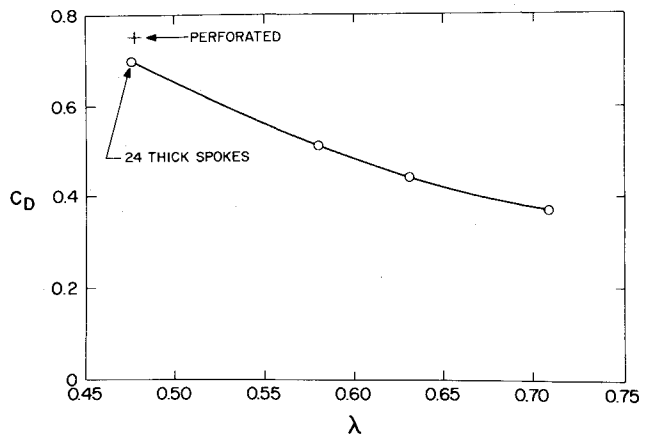

Fig. 6 Drag coefficient vs geometric porosity.

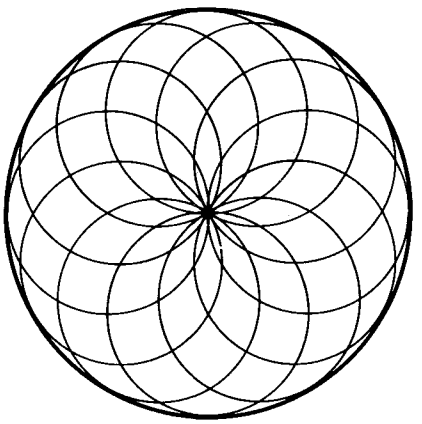

Fig. 8 "Optimal" network of the filamentary disk.

This formula expresses the torque coefficient (at a given Mach number) as a function of a single variable parameter, Reynolds number of the disk. The constant "a" depends primarily on the geometrical pattern of the disk while the constant "b" is determined mostly by the porosity λ. For the cases investigated here, the approximate values of the constants a and b are given in Table 1.

Table 1 Constants a and b for the tested disks

	a	b
Perforated disk	−1.77	1.2×10^{10}
Disks with thick spokes	−1.13	1.8×10^{6}–1.1×10^{7}
Disks with thin spokes	−1.08	3.3×10^{6}

Drag measurements are presented in Fig. 6 as a function of porosity λ. In a broad sense, the same geometric factors which increase the turning moment, also increase the drag for a configuration of not a very low porosity; hence, some general similarity can be observed between the trends shown in Figs. 4 and 6. However, when the moment coefficient depends strongly on rotation, the drag coefficient was found to be nearly constant, independent of ω. The drag coefficient was dominated by the geometric porosity λ. The perforated disk and the one with 24 thick spokes differed radically in geometrical arrangement of the surface, yet the difference in C_D is relatively small, as both configurations have almost identical λ. If we take into account that the effective porosity of the perforated model was actually lower due to limited effectiveness of the small holes close to the center of the model, then the difference in C_D becomes even less significant.

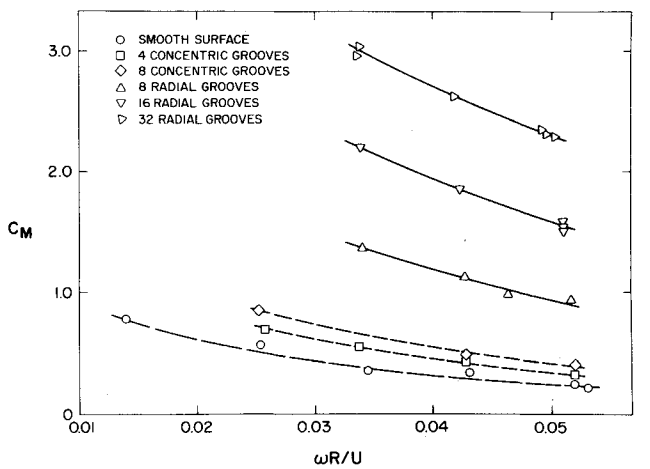

Fig. 7 Torque coefficient vs spin rate parameter; solid wall disks.

Solid Configurations

Figure 7 presents C_M vs $\omega R/U$ for the solid disk models. For a solid configuration, the flow separation occurs at the edge of the disk and the "stagnant" gas behind the disk partly rotates with the disk and contributes very little to the torque. Any such contribution may be, at least to the first approximation, omitted. The torque of a rotating disk is closely related to parameters of the boundary layer on the leading surface. These parameters depend strongly on the rotation ω and, of course, on the facial configuration of the surface. The torque can be written as

$$M_d = -(2\pi/\sin\phi) \int_o^R \tau_{z\theta} r^2 dr,$$

where $\tau_{z\theta} = \mu(\partial v/\partial z)_o$ denotes the circumferential component of the shearing stress. With circumferential grooves, $(\partial v/\partial z)_o$ is affected only indirectly, through an influence of the grooves on the radial flow of the boundary layer. This results in a relatively small increase of the friction torque when compared with a smooth surface. Conversely, radial grooves, which are perpendicular to v, affect the velocity gradient $(\partial v/\partial z)_o$ directly (and very strongly). Therefore, the corresponding values of C_M increase rapidly, approximately in proportion to the number of grooves. It is reasonable to expect that any facial deformations arranged in the circumferential direction (radial slots, channels, grooves, etc.) will result in a higher increase of the torque than that obtained with similar perturbations oriented radially. Since the same trend must take place for porous surfaces, we may formulate some suggestions concerning an aerodynamically desirable network configuration of a spinning filamentary decelerator. As the contribution to the torque of a ring element increases with a distance from the center, hence an optimal network should consist of fiber paths becoming increasingly circumferential oriented as they approach the outer diameter (Fig. 8).

In this investigation the measurements taken for solid grooved disks were carried out over a relatively narrow range of spin rate. Consequently, not enough data were collected to present torque coefficient as a function of Reynolds number. The drag coefficient of solid surface disks was constant, independent of rotation. This result is connected with the fact that separation occurs at the edge of the disk and is unaffected by the rotary motion. At very high spin rates, however, a small drag increase may be expected due to an increase of skin friction and possibly due to a slight decrease in base pressure (as a result of the centrifugal effects).

Conclusions

A wind-tunnel investigation of the flowfield and torque characteristics of several spinning disk models at $M = 4$ indicated conclusions as follows:

1) The torque coefficient for porous configurations decreases parabolically with angular velocity at rates depending on the geometry of the surface. For a given Mach number and over a fairly large range of angular velocity, C_M can be approximately expressed as a function of a single variable parameter, Reynolds number related to the peripheral velocity of the disk. This dependence takes the form $C_M = b(Re_d)^a$, where a and b are constants which depend on the geometry of the disk. For a selected geometric configuration, C_M is inversely proportional to the surface porosity.

2) For solid wall disks, torque increases rapidly due to any facial deformations (deformations from a smooth surface) arranged in the circumferential direction (for instance radial grooves, slots, etc.) and is roughly proportional to the total number of these deformations on the surface (assuming the deformations are of the same shape). Radially oriented perturbations (i.e., circumferential grooves, slots, etc.) produce relatively low torque increase. Since the same trend must take place for porous surfaces, hence a low-torque configuration of a spinning filamentary decelerator should consist of fibers whose paths become increasingly circumferential oriented as they approach the outer diameter. A disk with such a network may have a relatively low torque, while retaining high drag and radiation cooling capabilities. At the same time, this pattern appears to be compatible with the uniform stress requirements for the disk (isotensoid disk). It may also provide a good support for components and objects to be mounted around the periphery of the disk (small rocket motors, vanes, etc.).

3) Drag measurements indicate that for a given cone angle of a porous disk, C_D depends mainly on the geometric porosity and only to a small degree on the geometric pattern of the surface (at least as long as the "mesh size" is of the same order). The drag coefficient of any given configuration remained approximately constant, independent of rotation employed in these experiments.

References

[1] Schuerch, H. U. and MacNeal, R., "Deployable Centrifugally Stabilized Structures for Atmospheric Entry From Space," CR-69, 1964, NASA.

[2] Kyser, A. C., "The Rotornet: A High-Performance Hypersonic Decelerator for Planetary Entry," CR-247, 1965, NASA.

[3] Kyser, A. C., "The Uniform Stress Spinning Filamentary Disk," CR-106, 1964, NASA.

[4] MacNeal, R. H., "Mechanics of a Coned Rotating Net," CR-248, 1965, NASA.

[5] Shaw, M. C. and Macks, E. F., *Analysis and Lubrication of Bearings*, 1st ed., McGraw-Hill, New York, 1949, Chap. 10.